

Ray Tracing Simulations of a Novel Low Concentrator PVT Solar Collector for Low Latitudes

Diogo Cabral¹, João Gomes^{1,2}, Paul-Antoine Dostie-Guindon³, Björn Karlsson¹

¹ University of Gävle, Gävle (Sweden)

² Solarus Sunpower Sweden AB, Gävle (Sweden)

³ Ecole Polytechnique Montréal, Montréal (Canada)

Abstract

One way to reduce solar collector's production costs is to use concentrators that increase the output per photovoltaic cell. Concentrating collectors re-direct solar radiation that passes through an aperture into an absorber. The current study evaluates electrical performance of symmetric C-PVT solar collectors with a vertical bifacial receiver, through a numerical ray tracing model software, Tonatiuh. Several designs have been analysed, such as the Pure Parabola (PP) and MaReCo CPC geometries, both symmetric. Parameters such as concentration factor, electrical performance, transversal and longitudinal IAM (Incidence Angle Modifier), the influence of optical elements and influence of the length of the reflector in the shadow effect have been studied for different geometries. The simulations were performed for Mogadishu, Somalia and showed good results for the Pure Parabola collector (PPc) annual received energy, 379 and 317 kWh/m²/year for a focal length of 15 e 30 mm, respectively. A symmetrical double MaReCo CPC collector has been simulated with the annual received energy of 315 kWh/m²/year. The addition of the optical elements will decrease the annual received energy of the PPc by around 11.5%, where the optical properties (7.1%) and glass (4.1%) have the biggest impact in the annual received energy. Overall, symmetric geometries proved to be the most suitable geometries for low latitudes applications, being the geometry *f1* (focal length of 15 mm) the best one.

Keywords: Symmetric C-PVT, Pure Parabola collector, MaReCo CPC geometry, Tonatiuh.

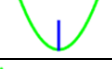
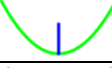
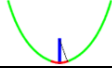
Quantity	Symbol	Unit
Acceptance angle	θ_c	degrees
Incidence angle	θ_i	degrees
Focal length	f	mm
Receiver height	Hr	mm
Aperture	$x_{m\acute{a}x}$	mm
Reflector height	z	mm
Aperture area	ApI_{area}	m ²
Solar irradiance	I_a	W/m ²
Concentration factor	Ci	-

1. Introduction

PVT systems can be based on Compound Parabolic Collector (CPC) (C-PVT) or on flat plate solar thermal collectors (PVT's) [1]. PVT collectors are hybrid solar collectors that simultaneously generate electrical (through PV cells) and thermal energy (through the solar radiation absorbed by the PV cells that is not converted into electricity). Since the efficiency of PV cells is temperature dependent, it is necessary to remove the excess heat. Previous studies showed that for every degree increase in temperature, the PV cell decreases around 0.45% [2]. This leads to a significant efficiency drop since PV cells can reach very high temperatures in summer [3], [4].

In order to carry the excess thermal energy generated by the PV cells, a cooling fluid is used (generally water), which leads to a decrease of the temperature of the solar cells, 'increasing' their overall efficiency. The waste heat harvested by the cooling fluid can be used as a cogenerated product and for heating applications [3]. This study will address different sets of simulations on symmetric low concentrator PVT geometries (with a vertical bifacial receiver), namely Pure Parabola (*f1* and *f2* geometry) and MaReCo CPC. Table 1.1 shows the main characteristics of the simulated reflector geometries, where the concentration factor, reflector height and focal length are shown.

Table 1.1. Geometry characteristics.

		Concentration factor (C_i)	Reflector height (z) [mm]	Focal length (f) [mm]
$f1$		1.2	75	15
$f2$		1.7	75	30
MaReCo CPC ¹		1.6	75	30

¹The MaReCo CPC geometry has an arc circle angle of 20° and a parabolic section with a focal length of 30 mm.

1.1 Concentrator Solar Panels

Solar energy technologies, just like any energy technologies, aim at providing energy at the lowest possible cost. This can be reached by increasing the efficiency or decreasing the investment cost. Concentrating collectors re-direct solar radiation that passes through an aperture into the receiver or absorber. These type of systems usually have a tracking system in order to maximize the energy yield [5]. Concentrating collectors are normally categorized on the field technology used, high or low concentration. The low concentration is categorized in three different categories such as (i) Booster reflector; (ii) Compound Parabolic Concentrator; (iii) Luminescent Concentrator. The high concentration technologies currently available are (i) parabolic trough collector; (ii) Linear Fresnel reflector; (iii) Central receiver (Tower); (iv) Parabolic Dish [6]-[8].

1.2 Compound Parabolic Collectors

CPC (Compound Parabolic Collectors) are non-imaging concentrators that do not require tracking system due to the ability to reflect all available beam radiation to the receiver. The incidence angle for these concentrators makes them very attractive from the point of view of system simplicity, flexibility and cost-effectiveness [9]. CPCs combine two parabolic reflectors (symmetric or asymmetric), each one of them with its own focus length (F , the focus of the right-hand parabola in Figure 1.1) at the lower edge of the other parabola [10], shown in Figure 1.1. The angle between the axis of the collector and the line connecting the focus of one of the parabolas with the opposite edge of the aperture is called acceptance half-angle (θ_c) [14].

The relationship between the size of the aperture ($2a$), the size of the receiver ($2a'$) and the acceptance half-angle is expressed through the following Equation 1.1 [10]:

$$2a' = 2a \sin\theta_c \quad (\text{eq. 1.1})$$

Knowing the concentration ratio is possible to obtain the relationship between the concentration ratio and the acceptance angle [10]:

$$C_i = \frac{2a}{2a'} = \frac{1}{\sin\theta_c} \quad (\text{eq. 1.2})$$

Other useful equations that describe the design of CPC concentrators are shown below. The following equations relate the focal distance of the side parabola to the acceptance half-angle (θ_c), receiver size, and height of the collector (h) [10]:

$$f = a'(1 + \sin\theta_c) \quad (\text{eq. 1.3})$$

$$h = \frac{f \cos\theta_c}{\sin^2\theta_c} \quad (\text{eq. 1.4})$$

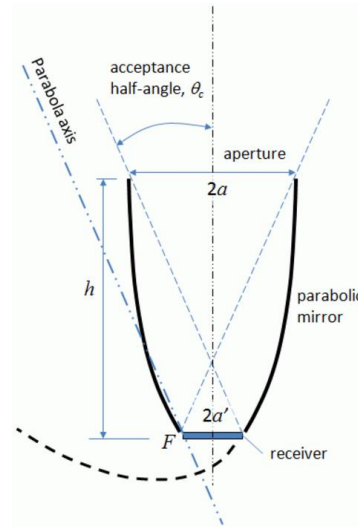


Figure 1.1. Cross section of a symmetrical non-truncated CPC [10].

These types of concentrators are made for each ray with an angle θ that comes into the CPC aperture with an angle smaller than θ_c to be reflected to the receiver at the base of the collector. The ray will be reflected back to the atmosphere, if the angle θ is greater than θ_c , as shown in Figure 1.2 [10].

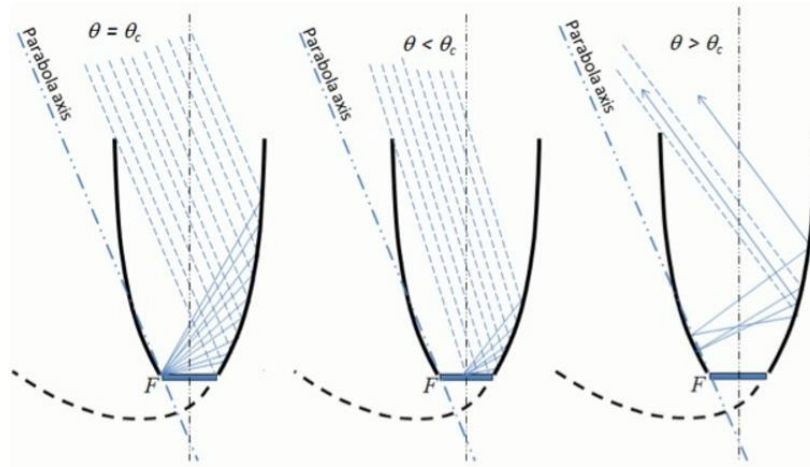


Figure 1.2. Reflection of the light rays directed to the CPC concentrator, at different angles [10].

1.3 Concentration with parabolic reflector

Different reflector geometries (symmetric) have been simulated in a ray tracing software, Tonatiuh. The simulated geometries are composed of either a full parabolic section or an arc circle with a parabolic section, thus, the importance of analysing the geometrical shape of these reflectors. For each point of the parabola, the distance between DR and RF is the same. Figure 1.3 shows the distance (VF) between the vertex and the focus of the parabola, known as focal length (f). The parabola axis intercepts the directrix and the focus, dividing the parabola into two symmetrical parts.

The following Equation 1.5 allows the calculation of the half aperture (x) in function of the reflector height (z) and the focal length (f) [4], [13].

$$x = \sqrt{f \times 4 \times z} \quad (\text{eq. 1.5})$$

All incoming light rays parallel to the axis of the parabola will be reflected the focus area, by definition of the focal point of the parabola. The ideal location of the receiver can be given as the focal point position, assuming that the light rays that arrive at the reflector surface are essentially parallel light rays, as shown previously in Figure 1.3.

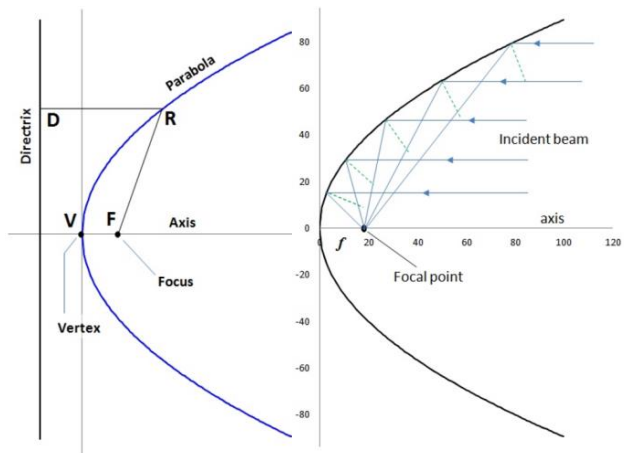


Figure 1.3. Parabola's geometry shape (left) and parallel incident beam rays (right) [11].

2. Methods

A thorough literature review in the field on reflector geometries and PVT technologies was carried out. Several sets of ray tracing simulations have been performed and posteriorly analyzed in Matlab. Below a short description of the procedure is presented.

- Literature review on symmetric and asymmetric reflector geometries and PVT technologies.
- Based on the literature review, two symmetric reflector geometries, Pure Parabola (PP) and MaReCo CPC geometries with a vertical bifacial receiver were selected:
 - Pure Parabola $f1$ [focal length of 15 mm].
 - Pure Parabola $f2$ [focal length of 30 mm].
 - MaReCo CPC [arc angle: 20°; focal length of 30 mm].
- Ray tracing simulations were performed for Mogadishu, Somalia (Latitude 2.04°, Longitude 45.31°) using a ray tracing software called Tonatiuh. The goal was to obtain the concentration factor, annual energy output, IAM (both transversal and longitudinal), the influence of optical elements (geometry $f2$), shadow effect (geometry $f1$ and $f2$) and non-electrical area of the receiver.
- Analysis of the results was performed in a multi-paradigm numerical computing environment software, called Matlab.
- A comparison between the different geometries was established.

The ray tracing simulations were set for a location near the equator (low latitudes), Mogadishu, Somalia (Latitude 2.04°, Longitude 45.31°) in order to study different geometries that work at these latitudes. No meteorological files or historical years were used during the simulations.

2.1 Tonatiuh

For the analysis and design of solar concentrating systems, a Monte Carlo ray tracer software was used. Principles of geometrical optics are used as a statistical method to get a complete and statistically analysis of an optical system, studying the route of a ray of light as it passes through the optical system. It creates an accurate and easy use of Monte Carlo ray tracer, simplifying the optical simulation of almost any type of solar reflector system. The rays are generated in a light source that simulates the sun and then these ray's intersections with system surfaces are calculated. The sunlight is defined by the sun position, i.e. the elevation and the azimuth. These two parameters can also be calculated as a function of the day, the hour, the latitude and the longitude. In order to simulate an entire year, the program has the possibility to input a script for parametrical simulations allowing to launch several simulations by means of a few loops in a script file that was created in Matlab (a multi-paradigm numerical computing environment software). After the simulations, the data is exported to Matlab in order to analyze the data.

The optical properties of the different collector elements were considered non-ideal (losses were taken into account), that is, the different characteristics of the materials, such as reflector reflectivity (92%), glass and gable transmittance (96% and 90%, respectively) were introduced in the software. Each simulation had 10 000 rays and the direct irradiation set as 1 000 W/m².

2.2 Software and simulation limitations

Regarding the software used for the sets of simulations, some limitations were found while the simulations were being performed, such as:

- Tonatiuh simulates the rotation of the 'sun' around the collector as 360° in longitudinal and transversal directions over a day. This meant that is needed to set the sunrise and sunset to 6 am to 6 pm, respectively in order not to have night output. The sunset and sunrise differ from day to day around 30 minutes throughout the year in Mogadishu. Tonatiuh can only store 24 cells (corresponding to 24 hours per day), therefore it was necessary to select by hours, leading to a slight inaccuracy. The error is not relevant since the annual received energy at low angles is significantly lower.
- No meteorological data has been inserted in the ray tracing simulation tool.
- The software does not take into account the cooling factor of solar cells from the working fluid (PV cell temperature dependence).
- PVT system losses and cell efficiency are not taken into account in Tonatiuh.

2.3 Reflector shape selection

Regarding the Pure Parabola geometries, each set of simulations, the reflector height (z) was fixed at 75 mm and the focus length (f) varied between 15 and 30 mm. After the first set of simulations (with a focal length of 15 mm and reflector height of 75 mm), the focus length was increased to 30 mm and fixed (being the reflector height constant during the whole simulation). This procedure was made for reflector height of 75 mm, and for a focal length of 15 and 30 mm [12]. The simulations were performed for Mogadishu, Somalia (Latitude 2.04° , Longitude 45.31°). The geometry ($f1$) is composed of a focal length (f) of 15 mm, reflector height (z) of 75 mm and a low concentration factor ($C_i= 1.2$). The additional geometry ($f2$) has a $C_i= 1.7$, $f= 30$ mm and $z = 75$ mm.

In order to get a good perspective of how the PPg (Pure Parabola geometry) performs, a different geometry has been simulated. The simulation was performed for a symmetrical MaReCo CPC with a concentration factor of 1.6, an arc circle angle of 20° and a reflector height of 75 mm. The focal length of the parabola section and the reflector height were set in line with the $f2$ geometry. Figure 2.1 shows a symmetrical MaReCo CPC geometry based on the MaReCo geometry. The receiver dimensions were set to fit this geometry (QQ'). The section of the concentrator between P_o and $P'o$ (red section in Figure 2.1) is an arc of a circle centred on Q . Section $A'P'o$ and AP_o (green section in Figure 2.1) is a parabola with focus at Q and axis $QP'o$. θ_i is the half-acceptance angle and θ_c is the arc circle angle.

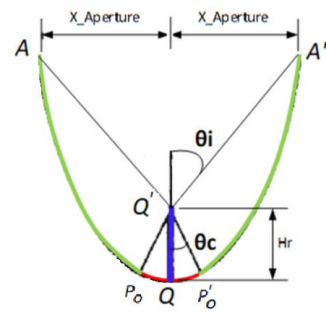


Figure 2.1. The optimum symmetrical MaReCo CPC.

2.4 IAM

The Incidence Angle Modifier (IAM) is the variance in output performance of a solar collector as the angle of the sun changes in relation to the surface of the collector. The longitudinal and transversal IAM can be obtained through the overall and optical efficiency, and aperture area (Apt_{area}). These values were collected from a Matlab script. The aperture area for receiver side is given by the following Equation 2.1.

$$Apt_{area} = \left(\sqrt{z \times 4 \times f - \frac{thickness_{receiver}^2}{2}} \right) \times Length_{receiver} \quad (eq. 2.1)$$

The aperture area allows the calculation of the overall efficiency of the collector [4].

$$Eff(\theta_i) = \frac{Power(\theta_i) [W]}{I_a [W/m^2] \times Apt_{area} [m^2]} \quad (eq. 2.2)$$

Where the Power (θ_i) is given by Tonatiuh and I_a is the solar irradiance that passes through the collector aperture, with a value of $1\ 000 [W/m^2]$.

The optical efficiency (η_{opt}) is given by the maximum value of Equation 2.3.

$$\eta_{opt} = \max(Eff(\theta_i)) \quad (eq. 2.3)$$

With all the parameters obtained, the transversal and longitudinal IAM is obtained using Equation 2.4.

$$IAM(\theta_i) = \frac{Eff(\theta_i)}{\cos(\theta_i) \times \eta_{opt}} \quad (eq. 2.4)$$

Where θ_i are the angles $[-90^\circ, -89^\circ, -88^\circ, -87^\circ, -86^\circ, 85^\circ, \dots, 85^\circ, 86^\circ, 87^\circ, 88^\circ, 89^\circ, 90^\circ]$. The interval between angles was set in order to achieve a more accurate data.

2.5 Influence of the optical elements

In order to get a more precise knowledge of how the different elements affect the annual received energy of these kind of collectors, the influence of the optical elements such as (i) frame; (ii) glass; (iii) gables; (iv) receiver thickness; (v) optical properties were studied. The simulations consisted by adding the different elements to geometry $f2$ and visualize their influence in the annual received energy.

2.6 Shadow effect

The effect of the shadow in the annual received energy was studied, by increasing the reflector length. Consisted by adding progressively length to the reflector, in order to reduce the shadow on the receiver. The receiver length was set as constant and the reflector area was gradually increased by 0.02, 0.04 and 0.06 m².

2.7 Electrical non-active area

The electrical non-active area gives the percentage of receiver area that does not produce electricity. In order to improve the performance of the collector, it is necessary to improve the performance of the receiver, by reducing the electrical non-active area. A study has been conducted in order to find the electrical non-active area of the selected receiver. The electrical non-active area was removed and after the annual received energy has been updated.

3. Results

3.1 Maximum efficiency and yearly energy output

This section presents the main results for an annual receive energy and a 3D view of the maximum efficiency at each angle. The vertical bifacial receiver is composed of side A (receiver side facing north) and side B (receiver side facing south).

3.1.1 Pure Parabola f1 collector

From the ray-tracing software, it was possible to extract the data to a Matlab script and run it, in order to get the annual received energy from both receivers A and B. This geometry receives an annual received energy of 2 186 kWh/m²/year. The presented value is obtained by using a scale factor of 3.2, due to the fact that the simulated collector has 0.31 m².

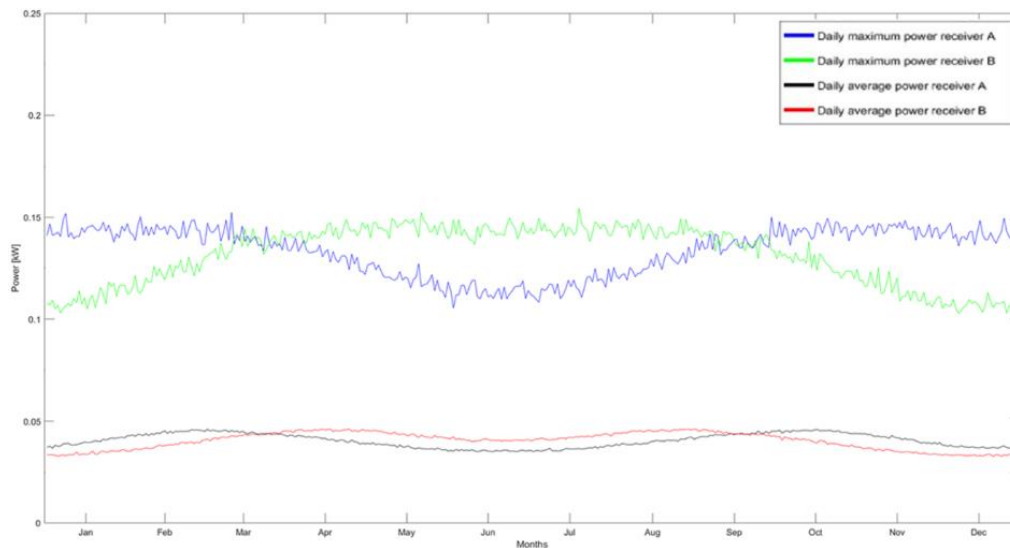


Figure 3.1. Daily maximum and average power output for the *f1* collector.

The receiver B will have higher annual received energy during the months of March-September, due to the fact that the sun will be on the north side of the collector. On the remaining months, the receiver A will have a higher annual received energy from September-March, when the sun is on the south side of the collector.

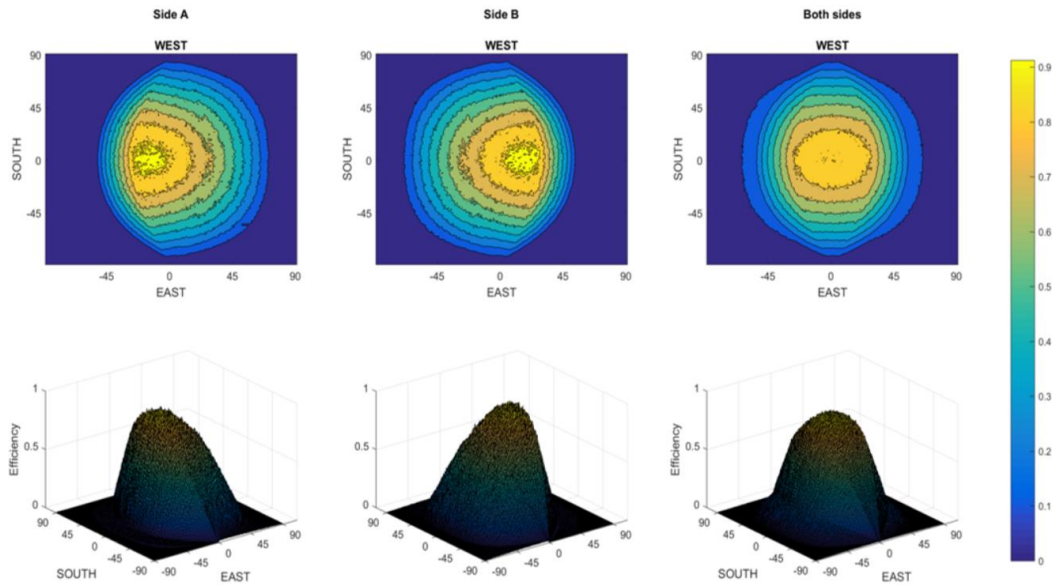


Figure 3.2. 3D view of the maximum efficiency at each angle (transversal and longitudinal) for the $f1$ collector.

The distribution of the solar radiation is more evenly distributed across both receivers since they produce around the same. The maximum efficiency value is slightly above 90%. The collector performance (daily average power) throughout the year is in line with the average seasonal variation of the daily extra-terrestrial solar radiation for horizontal surfaces at low latitudes.

3.1.2 Pure Parabola $f2$ collector

This geometry receives an annual received energy of 1 831 kWh/m²/year, with a scale factor of 2.3, for a simulated collector area of 0.44 m². Due to its concentration factor (bigger aperture), this geometry does not have the same properties as the one described above, since it has a different capacity to reflect the rays with the same accuracy as the geometry presented previously ($f1$ geometry).

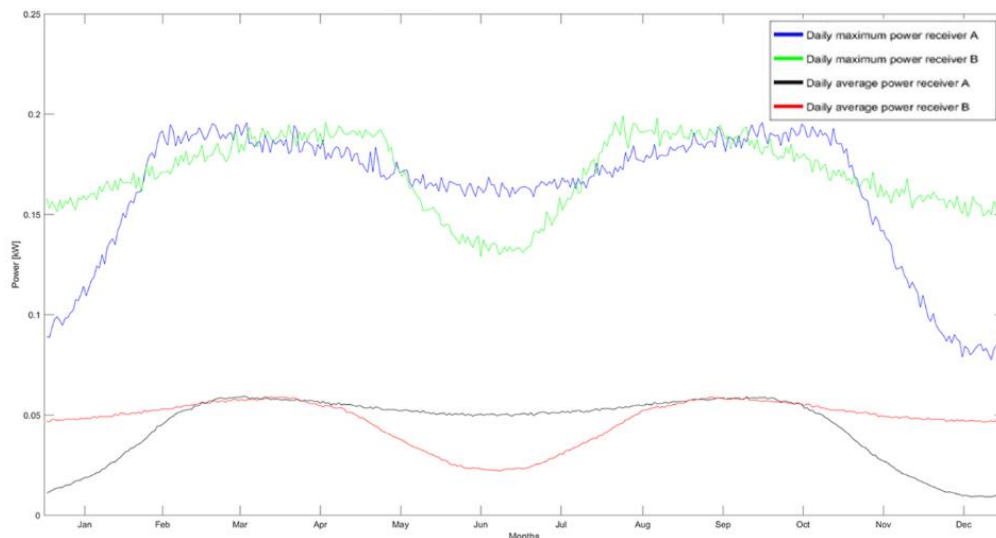


Figure 3.3. Daily maximum and average power output for the $f2$ collector.

The receiver B has a higher annual received energy during the months of November-February, March-May and July-September, due to the fact that the sun is on the north side of the collector. On the other hand, the receiver A has a higher annual received energy during the months of February-March, May-July and September-November when the sun is on the south side of the collector.

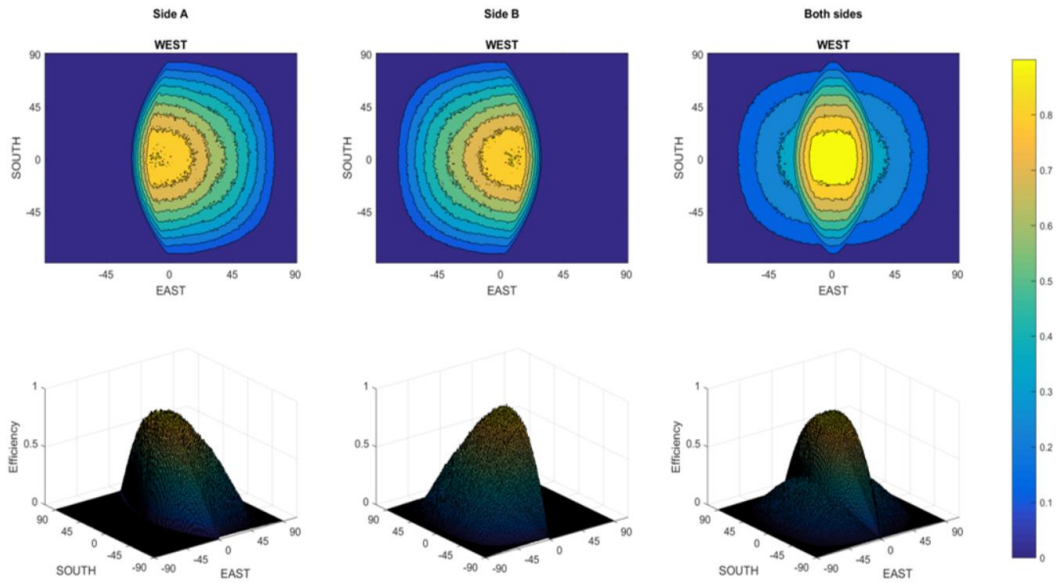


Figure 3.4. 3D view of the maximum efficiency at each angle (transversal and longitudinal) for the f_2 collector.

The maximum efficiency value is slightly below 90%. As f_1 geometry, this collector performance (daily average power) throughout the year is in line with the average seasonal variation of the daily extra-terrestrial solar radiation for horizontal surfaces at low latitudes.

3.1.3 MaReCo CPC geometry

A value of 1 819 kWh/m²/year was obtained for this reflector shape, by using a scale factor of 2.4, due to the fact that the simulated collector has 0.42 m².

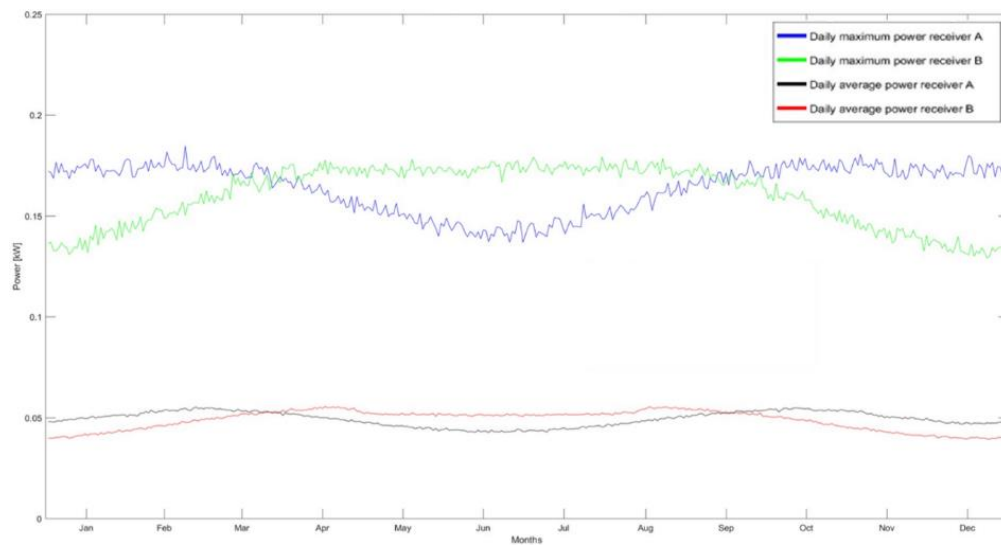


Figure 3.5. Daily maximum and average power output for the MaReCo CPC geometry.

The receiver B will have higher annual received energy during the months of March-September, due to the fact that the sun will be on the north side of the collector. On the remaining months, the receiver A will have a higher annual received energy from September-March, when the sun is on the south side of the collector.

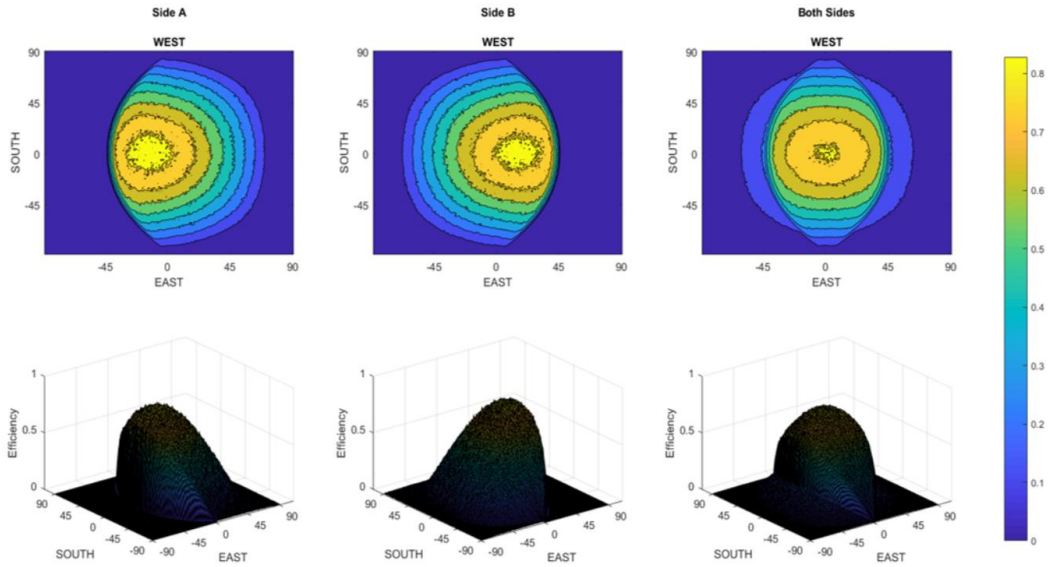


Figure 3.6. 3D view of the maximum efficiency at each angle (transversal and longitudinal) for the MaReCo CPC geometry.

Despite having a similar annual received energy as geometry *f2*, the maximum efficiency range of this geometry is bigger than in geometry *f2*, with a value slightly above 80%.

3.2 IAM

3.2.1 Pure Parabola *f1* collector

Figure 3.7 shows the normalized maximum efficiency working range for the PPc *f1*, around [-30°S, 30°N].

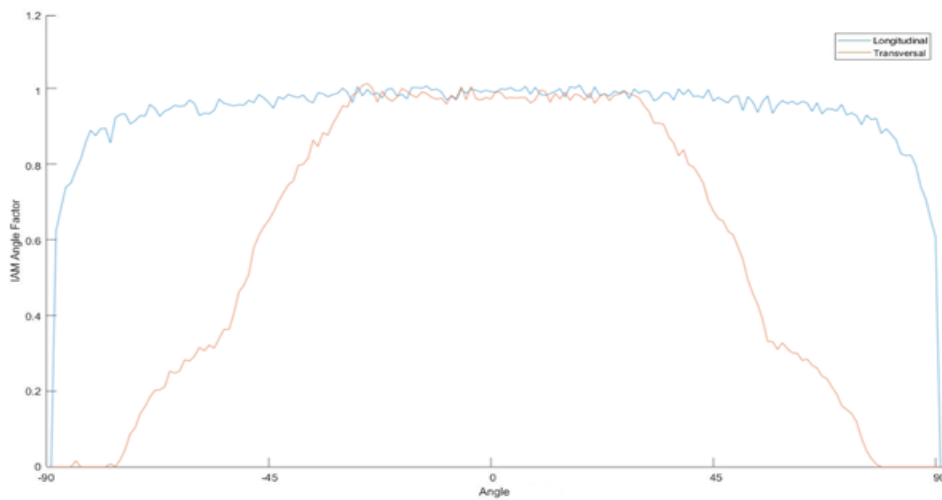


Figure 3.7. IAM transversal and longitudinal for both receiver sides, *f1* collector.

This geometry has the ability to re-direct efficiently the sun rays towards the receiver, due to the fact that the angles θ that comes into the CPC aperture with an angle smaller than θ_c (acceptance half-angle) will be reflected more efficiently into the receiver.

3.2.2 Pure Parabola $f2$ collector

Figure 3.8 shows the normalized maximum efficiency working range for the PPc $f2$, around $[-15^{\circ}\text{S}, 15^{\circ}\text{N}]$.

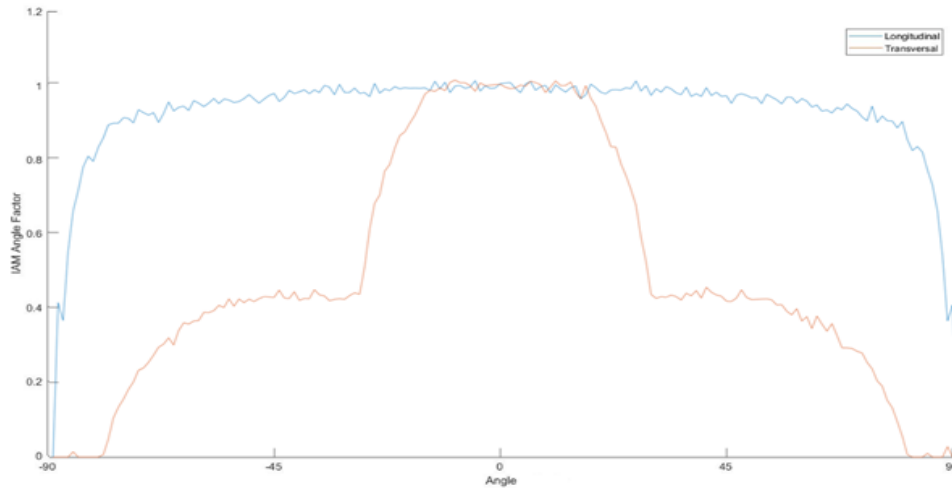


Figure 3.8. IAM transversal and longitudinal for both receiver sides, $f2$ collector.

Comparing geometry $f2$ with $f1$, it is possible to verify that at some angles, geometry $f2$ has no ability to re-direct the incident rays to the receiver efficiently (steeper curve from $[-30^{\circ}\text{S}, -15^{\circ}\text{N}]$ and $[15^{\circ}\text{S}, 30^{\circ}\text{N}]$), since the angle θ is bigger (for a longer period than for geometry $f1$) than θ_c , thus lowering the maximum efficiency range. A narrower maximum efficiency range and lower maximum efficiency led to a lower annual received energy when compared with geometry $f1$.

3.2.3 MaReCo CPC collector

Figure 3.9 shows the normalized maximum efficiency working range for the symmetrical MaReCo CPC collector, around $[-40^{\circ}\text{S}, 40^{\circ}\text{N}]$.

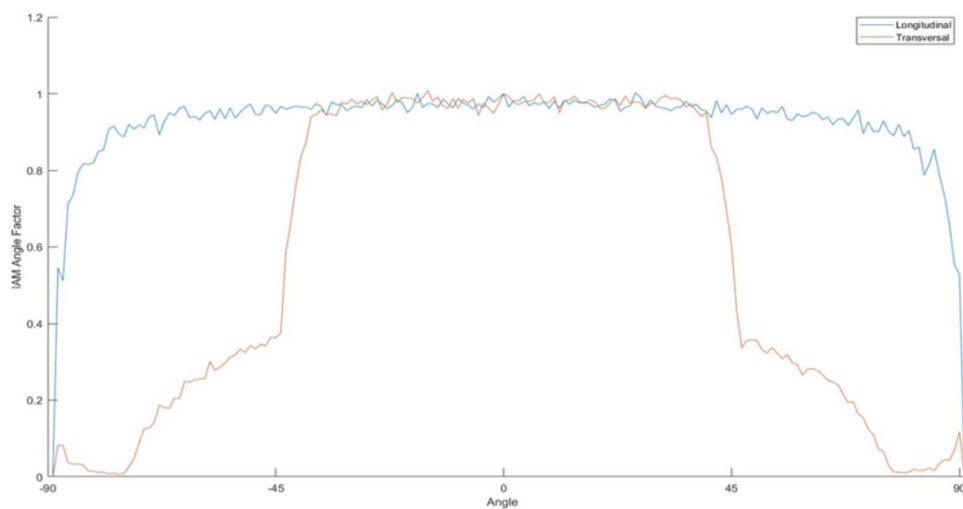


Figure 3.9. IAM transversal and longitudinal for both receiver sides, MaReCo CPC geometry.

The lower maximum efficiency value of this geometry is compensated by a wider maximum efficiency working range, when compared with geometry $f2$.

3.3 Influence of the optical elements in geometry f2

The PPg corresponds to the PPC without a frame, gable, glass, optical properties and a 2 mm receiver thickness.

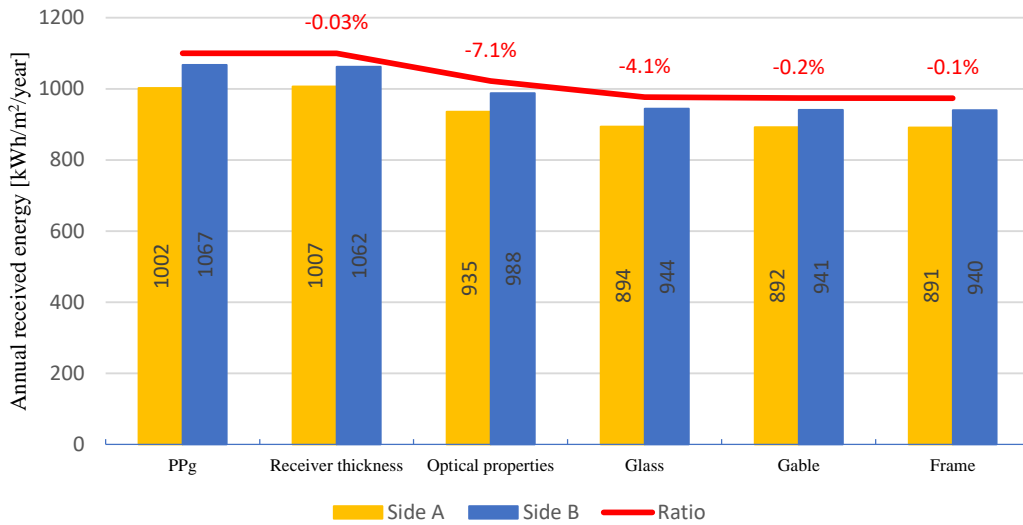


Figure 3.10. Results of the influence of the optical elements and properties in the geometry f2.

Figure 3.10 shows that the optical properties and glass have the biggest impact on the electrical performance of the collector. On the other hand the receiver thickness, gable and frame almost have no influence in the results, accounting for 0.3%. Overall, the difference between the geometry and the collector is around 11.5%. The energy production ratio between receiver sides decreases with the influence of the optical properties of the materials. Since the value of reflectivity was considered constant (normal to the collector) regardless the suns' altitude, the influence of the glass is lower. It is expected that the glass will have a bigger influence if this parameter is taken into account.

3.4 Shadow effect (Pure Parabola f1 collector)

Electricity costs were set as 0.211 €/kWh for households [12] and the reflector price was taken from a standard reflector with reflectivity of 98%. Table 3.1 shows the payback time for an increased reflector length.

Table 3.1. Payback time for an increased reflector length, geometry f1.

Additional area [m²]	Additional reflector price [€]	Production surplus [kWh/m²]	Payback [years]
+ 0.02	0.7	18	9.2
+ 0.04	1.5	20	8.9
+ 0.06	2.2	22	7.9

The payback time goes from 7.9 up to 9.2 years to start to pay off (breakeven point), showing that is not effective since the payback time is too big for such a small area. The presented values show that a longer reflector reduces the shadow effect, increasing the annual received energy.

3.5 Electrical non-active area

The electrical non-active area accounts for 12.1 % and the cell efficiency for 19.7%. The updated values for each collector are given in the following Table 3.2.

Table 3.2. Updated annual received energy per collector.

	Annual received energy [kWh/m²/year]	
	Tonatiuh	Updated
PP f1	2 186	379
PP f2	1 831	317
MaReCo CPC	1 819	315

4. Discussion

As expected, the $f1$ geometry has a wider transversal maximum efficiency working range as a result of its narrow aperture, when compared with $f2$ geometry. This geometry has the ability to re-direct more efficiently the sun rays towards the receiver. The transversal maximum efficiency working range of the PPc is around $[-30^\circ, 30^\circ]$ and $[-15^\circ, 15^\circ]$ for a focal length of 15 and 30 mm, respectively. On the other hand, the MaReCo CPC collector has a maximum efficiency working range around $[-40^\circ\text{S}, 40^\circ\text{N}]$.

The values for the annual received energy are, as expected, higher for the $f1$ collector (2 186 kWh/m²/year) than for the $f2$ collector (1 831 kWh/m²/year), especially as a result of its geometrical characteristics (lower concentration factor). Regarding the symmetric MaReCo CPC collector, the results show that this geometry has a slightly lower annual received energy than the $f2$ geometry. It was expected that this geometry would perform better than the $f2$ geometry, due to its lower concentration factor (fewer reflection losses). The MaReCo CPC collector has an annual received energy around 1 819 kWh/m²/year. Lower concentration means higher annual received energy, due to lower reflection losses.

Figure 3.10 shows that the glass and the optical properties have the biggest impact in the annual received energy of the $f2$ collector. The annual received energy for the symmetrical geometries can go up to 11.5%, showing that the optical properties of the different elements affect significantly the performance of these geometries.

Table 3.2 shows the annual received energy, considering a non-electrical area of 12.1% and a cell efficiency of 19.7%. The addition of these parameter led to an annual received energy of 379, 317 and 315 kWh/m²/year for the collector $f1$, $f2$ and MaReCo CPC, respectively.

Regarding the shadow effect, it is possible to acknowledge that increasing the reflector length is not effective, not only because at low angles (sunrise and sunset) the reflected sun rays will be reflected back to the atmosphere (the receiver is not long enough to collect the sun rays), but also due to the fact that the payback time for such small area can go from 8 to 9 years for such small area.

Overall, the simulated geometries showed potential for low latitudes applications, being the geometry $f1$ the best one. A way to validate the simulations would be the construction of a prototype and to perform CFD simulations in order to study the thermal potential of a C-PVT with these geometries.

5. References

- [1] O. Z. Sharaf and M. F. Orhan, "Concentrated photovoltaic thermal (CPVT) solar collector systems: Part I – Fundamentals, design considerations and current technologies," *Renewable and Sustainable Energy Reviews*, vol. 50, pp. 1500-1565, 10, 2015.
- [2] A. H. Jaaz *et al.*, "Design and development of compound parabolic concentrating for photovoltaic solar collector: Review," *Renewable and Sustainable Energy Reviews*, vol. 76, pp. 1108-1121, 9, 2017.
- [3] S. A. Kalogirou and Y. Tripanagnostopoulos, "Hybrid PV/T solar systems for domestic hot water and electricity production," *Energy Conversion and Management*, vol. 47, (18–19), pp. 3368-3382, 11, 2006.
- [4] S. R. Reddy, M. A. Ebadian and C. Lin, "A review of PV–T systems: Thermal management and efficiency with single phase cooling," *Int. J. Heat Mass Transfer*, vol. 91, pp. 861-871, 12, 2015.
- [5] William B Stine and Michael Geyer, Eds., *Power from the Sun*. (2001st ed.) 2009.
- [6] V. V. Tyagi, S. C. Kaushik and S. K. Tyagi, "Advancement in solar photovoltaic/thermal (PV/T) hybrid collector technology," *Renewable and Sustainable Energy Reviews*, vol. 16, (3), pp. 1383-1398, 4, 2012.
- [7] R. Abbas *et al.*, "Parabolic trough collector or linear Fresnel collector? A comparison of optical features including thermal quality based on commercial solutions," *Solar Energy*, vol. 124, pp. 198-215, 2, 2016.
- [8] R. Pujol-Nadal *et al.*, "Optical and thermal characterization of a variable geometry concentrator using ray-tracing tools and experimental data," *Appl. Energy*, vol. 155, pp. 110-119, 10/1, 2015.
- [9] L.A. Diwan, "Study of Optimizations in a Novel Asymmetric Photovoltaic/Thermal Hybrid Solar Collector", 2013.
- [10] M. Fedkin and A. Dutton, "CPC Collectors - concentration of diffuse radiation," 2015.
- [11] M. Fedkin and A. Dutton, "Concentration with a parabolic reflector," vol. 2017, (19 March), 2015.
- [12] 'Electricity and gas prices, second half of the year', 2013-15 (EUR per kWh), 2017.
- [13] R. Winston, R. Finkler and J. Shamir, "High Collection Nonimaging Optics," *6th Mtg in Israel on Optical Engineering*, vol. 1038, pp. 590-598, Dec-7, 1988.
- [14] W. T. Welford and R. Winston, "Chapter 4 - nonimaging concentrators: The compound parabolic concentrator," in *High Collection Nonimaging Optics*, W. T. WELFORD and R. WINSTON, Eds. Academic Press, 1989, pp. 53-76.